EFFECTIVE ELASTIC MODULI OF CLOSED-CELL ALUMINIUM FOAMS - HOMOGENIZATION METHOD

Petr Koudelka[1], Tomáš Doktor[1], Jaroslav Valach[1], Daniel Kytýř[2] and Ondřej Jiroušek[2]

During the last decades, there has been much effort on the determination of effective elastic properties of porous metals. In this paper, the overall elastic moduli of reference aluminium foam Alporas are assessed using predictive methods based on definition of compliance contribution tensor. Surface of the foam is captured using flatbed scanner and such data is subjected to image and signal processing routines in order to obtain dimensions of the sufficient representative volume element and calculation of structural characteristics for analytical homogenization. It is shown that from all considered homogenization models only the Mori-Tanaka scheme gives results reasonably close to nominal values.

Keywords: metal foam, micromechanical properties, homogenization
MSC2000: 53C 05.

1. Introduction

Metal foams are highly porous materials with cellular inner structure that were developed by mimicking microstructures identified in nature. Among other porous metals, aluminium metal foams find wide range of applications from deformation energy absorption to noise attenuation, where their lightweight character facilitates design of highly effective constructions.
During the last decades, there has been much effort to the determination of effective elastic properties of porous metals. Experimental approach by the means of uni-axial compression and tensile tests can be utilized to obtain elastic properties of metal foams. However due to random character of the material's inner structure

[1]Czech Technical University in Prague, Faculty of Transportation Sciences, Department of Mechanics and Materials, Na Florenci 25, 110 00 Prague 1, e-mail: xpkoudelka@fd.cvut.cz

[2]Czech Technical University in Prague, Faculty of Transportation Sciences, Department of Mechanics and Materials, Na Florenci 25, 110 00 Prague 1

[3]Czech Technical University in Prague, Faculty of Transportation Sciences, Department of Mechanics and Materials, Na Florenci 25, 110 00 Prague 1

[4]Academy of Sciences of the Czech Republic, Institute of Theoretical and Applied Mechanics, Prosecká 76, 190 00 Prague 9

[5]Academy of Sciences of the Czech Republic, Institute of Theoretical and Applied Mechanics, Prosecká 76, 190 00 Prague 9

extensive set of experiments has to be performed in order to obtain reliable results. Thus experimental determination may be very costly and time consuming. Alternatively several different methods based on finite element analysis of the material's microstructure may be introduced. This involves i) microstructural modeling using discretization [1], ii) models developed on the basis of a series of computed microtomography scans [2] and iii) numerical homogenization [3]. Generally all of these techniques retain economical disadvantages as highly specialized hardware and software is required. That is why analytical approach seems to be promising among other methods. Here effective elastic properties are usually assessed using relationships giving the variation of elastic constants in terms of porosity [4] or by analytical homogenization schemes based on various constitutive laws.
In this paper, the overall elastic moduli of reference aluminium foam Alporas are assessed using predictive methods (i.e. non-interaction approximation, differential scheme, etc.) based on definition of compliance contribution tensor.

2. Materials and methods

As an input data, surface of the foam (see Fig. 1) was captured using high resolution (4800 dpi) flatbed scanner and assessed image was subjected to image manipulation (segmentation) and analysis procedures in order to obtain structural characteristics (porosity, shape factors and aspect ratios of pores) for all further calculations. To obtain dimensions of the sufficient representative volume element (RVE), spectral analysis was applied on the segmented image data for determination of the most characteristic frequencies in the foam's random microstructure. Subsequently, periodicity of the microstructure was assessed and RVE dimensions were calculated. Homogenization procedure was utilized only on the macroscopic level of foam's hierarchical structure.

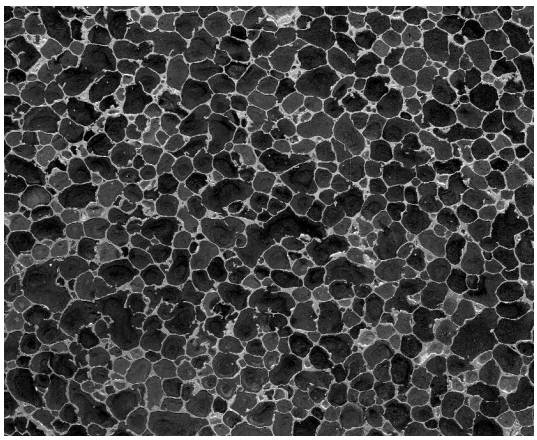

FIGURE 1. Captured macrostructure of Alporas

2.1. Alporas

Alporas® is a light-weight cellular material with closed-cell internal structure industrially produced since 1986. Practical production is conducted by Japan company Shinko Wire Co., Ltd. that is at the European market represented by Austrian reseller Gleich, Gmbh. Its macroscopic physical and mechanical properties are almost perfectly isotropic thanks to polyhedral cell shapes with outstanding three dimensional stability. Typical cell dimensions lie in interval $1 - 13$ mm whereas average dimension is 4.8 mm [5]. The foam typically exhibits 90 % porosity that can be controlled during the foaming process to certain level taking into account that polyhedral cells become spherical at porosities lower than 70 %.

3. RVE assessment

2-D image data captured using high resolution flatbed scanner were segmented to output in form of a binary image. In this image, path-lines were generated in order to define locally phase functions:

$$\phi(s) = s \in (x, y). \tag{1}$$

These phase functions represent the fundamentals for the spectral analysis to assess periodic character of the structure and dimensions of RVE [6]. In this paper, phase functions were generated and evaluated for every row and line in the binary array of captured foam's microstructure.
There are several ways to express mathematical basis of tools used for signal processing. For the purpose of this paper, a time history random signal function $x(t)$ has its corresponding autocorrelation function expressed by:

$$R_{\mathrm{xx}}(\tau) = \lim_{\mathrm{T}\to\infty} \int_0^{\mathrm{T}} x(t)\, x(t+\tau)\, \mathrm{d}t \tag{2}$$

where t and τ are time variables and T is the length of the time series. The power spectrum density (PSD) function $S(f)$ is then defined as the Fourier transform (FT) of the autocorrelation function:

$$S_{\mathrm{xx}}(f) = \int_{-\infty}^{\infty} R_{\mathrm{xx}}(\tau)\, e^{-2\pi i f \tau} \mathrm{d}\tau \tag{3}$$

where f is the signal frequency and coordinate of its maximum defines the investigated most characteristic period of the signal. This method can be also applied to other fields like in this paper the investigation of materials with random microstructure. Here, the phase function $\phi(s)$ is not a time history random field but depends stochastically on the spatial path variable s.

Therefore, the time variables t and τ in autocorrelation function and its corresponding PSD function are replaced by the spatial coordinates s and σ [7]:

$$R^*_{\mathrm{xx}}(\sigma) = \lim_{\mathrm{S}\to\infty} \frac{1}{\mathrm{S}} \int_0^{\mathrm{L_S}} \phi(s)\,\phi(s+\sigma)\,\mathrm{d}s, \tag{4}$$

$$S^*_{\mathrm{xx}}(f_{\mathrm{s}}) = \int_{-\infty}^{\infty} R^*_{\mathrm{xx}}(\tau)\, e^{-2\pi i f \sigma} \mathrm{d}\sigma \tag{5}$$

where L_{S} is the one-dimensional path length and f_{S} is the structural frequency in m^{-1}, which is reciprocal of the searched structural period. The PSD function is evaluated in order to detect large peaks (local and global extremes) that represent characteristic periods of the structure. Calculation of the PSD function for a limited signal/path length with discrete data points can be carried out by different spectral estimation procedures. In this study, the periodogram spectral estimation denoted by the following equation was used:

$$S^*_{\mathrm{xx}}(f_{\mathrm{s}}) = \frac{1}{L_{\mathrm{S}}} \left|\xi(f_{\mathrm{s}}, L_{\mathrm{s}})\right|^2 \tag{6}$$

where $\xi(f_{\mathrm{s}}, L_{\mathrm{s}})$ is the discrete Fourier transform (DFT) of the phase function $\phi(s)$ given by:

$$\xi(f_{\mathrm{s}}, L_{\mathrm{s}}) = \int_0^{L_{\mathrm{S}}} \phi(s)\, e^{-2\pi i f_{\mathrm{S}} s} \mathrm{d}s. \tag{7}$$

Value of global maximum can be used as the period magnitude for the current path function. However, the location of this maximum varies even for different paths within the same cross-section and especially for 2-D input data, high caution has to be given to treatment of stochasticity in all the calculations. Therefore, in order to get the reliable structural period in each structural direction, an average over all path-lines within a 2-D cut is made. Furthermore, the input image is divided into several square regions overlapping each other by one half of its area (see Fig. 2). This ensures that each segment of generated path-lines is in the calculation included no more than twice. Such network of several overlapping regions facilitates proper characterization of the random structure with required level of reliability of results. Hence, the value of investigated period is averaged over the defined cuts per structural direction among each region and then over all generated regions.

4. **Homogenization**

4.1. **Microstructural characterization**

Porosity of the material was determined by weighting of a set of samples resulting in a mean value of 91.4%. Then, the required microstructural information

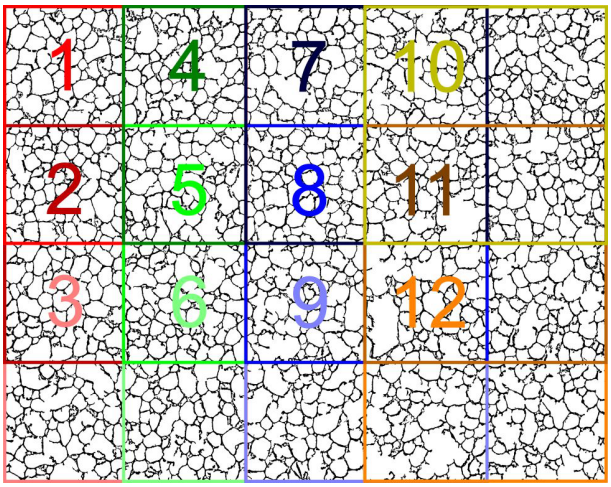

FIGURE 2. Example of proposed scheme of overlapping regions showing segmented structure of Alporas with twelve generated square shaped areas

was extracted from the binary image leading to determination of the average aspect ratio of 3-D pores according to the following formula [8]:

$$\gamma^{3D} = \frac{3}{2}R \tag{8}$$

where R is the 2-D shape factor of pores denoted by the following equation:

$$R = \frac{1}{A}\sum_{i} A_i \gamma_i^{2D} \tag{9}$$

γ_i^{2D} is the aspect ratio, A_i is the area of i-th 2-D pore and A is the total area of all pores.

4.2. Effective elastic properties

In case of elastic properties investigated here for inhomogeneous materials, all calculations are based on fourth rank tensors leading to quantification of two isotropic material constants (elastic modulus and Poisson's ratio) [9]. Relations described in this section are valid for effective Young's modulus of a material containing isotropic mixtures of non-spherical pores and used prediction schemes are rooted in the non-interaction approximation and compliance contribution tensor defined as [10]:

$$\varepsilon_{ij} = S^0_{ijkl}\sigma_{kl} + H_{ijkl}\sigma_{kl} \tag{10}$$

where the H-tensor depends on pore shapes and its elastic properties.

For ellipsoidal pores, it is related to Eshelby's tensor by [10]:

$$H = \frac{V_*}{V}\left[C^0 : (J - s)\right]^{-1} \tag{11}$$

where

$$C^0 = \left(S^0\right)^{-1}, \tag{12}$$

$$(J)_{\mathrm{ijkl}} = \frac{1}{2}\left(\delta_{\mathrm{ik}}\delta_{\mathrm{jl}} + \delta_{\mathrm{il}}\delta_{\mathrm{jk}}\right). \tag{13}$$

Its components are expressed in terms of elliptic integrals for ellipsoidal pores and reduced to elementary functions in case of spheroidal pores. Calculation of these tensors can reduce to quantification of factors from the following relation when explicit analytic inversion is introduced [11]:

$$H = \frac{V_*}{V}\frac{1}{G_0}\sum_{\mathrm{k}=1}^{6} h_{\mathrm{k}} T^{(k)}. \tag{14}$$

4.**2**.1. *Non-interaction approximation.* Here, the effective compliance tensor can be denoted as [12]:

$$S = S_0 + \sum_{\mathrm{i}} H^{(i)} = S_0 + H_{\mathrm{NI}} \tag{15}$$

where H_{NI} is in this case:

$$H_{\mathrm{NI}} = p\left[\frac{\frac{3B_1 - B_2}{2}}{G_0}\left(\frac{1}{3}II\right) + \frac{B_2}{G_0}\left(J - \frac{1}{3}II\right)\right]. \tag{16}$$

Shape factors B_1 and B_2 that are functions of aspect ratios and Poisson's ratio of the matrix material can be assessed by integration of (14) over all possible orientations resulting in:

$$B_1 = \frac{26h_1 + 3h_2 + 28h_3 + 4h_5 + 6h_6}{30}, \tag{17}$$

$$B_2 = \frac{2h_1 + 11h_2 - 4h_3 + 8h_5 + 2h_6}{30} \tag{18}$$

where coefficients h_{i} are yielded by the explicit analytic inversion of the H-tensor.

The effective Young's modulus is using this scheme predicted by the following relation:

$$E = \frac{E_0}{1 + p\xi(\gamma, \nu_0)} \tag{19}$$

where

$$\xi(\gamma, \nu_0) = 2(1 + \nu_0)\left(B_1 + \frac{B_2}{2}\right). \tag{20}$$

4.**2**.2. *Self-consistent scheme.* Self consistent scheme leads to a system of two non-linear equations for the bulk and shear moduli [13]:

$$K = K_0\left[1 - p\frac{2(1+\nu)}{1-2\nu}\left(\frac{3B_1(\gamma,\nu) - B_2(\gamma,\nu)}{2}\right)\right], \tag{21}$$

$$G = G_0\left[1 - 2pB_2(\gamma,\nu)\right]. \tag{22}$$

Using solution of a relation obtained by dividing the (21) by (21), the effective Young's modulus can be obtained from:

$$E = E_0\left[1 - p\xi(\gamma,\nu)\right]. \tag{23}$$

4.**2**.3. *Differential scheme.* Differential scheme is usually interpreted as an infinitesimal form of the self-consistent scheme which leads to a system of two differential equations for both the bulk and shear moduli [14]. Detailed analysis of these relations for spheroidal inclusions is given in [15] and the solution leads to the effective Young's modulus expressed as:

$$E = E_0 \exp\left(-\int_0^p \frac{\xi[\gamma, \nu(\rho)]}{1-\rho}\mathrm{d}\rho\right). \tag{24}$$

If one considers the negligible variation of Poisson's ratio with porosity relationship (24) reduces to:

$$E = E_0(1-p)^{\xi(\gamma,\nu)}. \tag{25}$$

4.**2**.4. *Effective-fields method.* The Mori-Tanaka [16] and Levin-Kanaun [17] single equation schemes are ranked among effective fields method and appear in the following expressions for the effective Young's modulus:

$$E = \frac{E_0}{1 + \dfrac{p\xi(\gamma, \nu_0)}{1-p}}, \tag{26}$$

$$E = \frac{E_0}{1 + \dfrac{p\xi(\gamma, \nu_0)}{1 - p\dfrac{\xi(\gamma, \nu_0)}{\xi(1, \nu_0)}}}. \tag{27}$$

5. **Results**

Using the methods discussed hereinbefore, mechanical properties of Alporas closed-cell aluminium foam were assessed. By analyzing scanned macrostructure of the foam, dimensions of the RVE were obtained by methods of spectral analysis:

$$\begin{aligned} x &= 28.84\,\text{mm}, \\ y &= 29.45\,\text{mm}. \end{aligned}$$

Then 3-D shape factor resulting in value $\gamma^{3D} = 0.674$ was calculated as input to the homogenization models. Tab. 1 summarizes obtained homogenized effective elastic moduli.

Table 1. Results from the homogenization schemes

Scheme	$E_{\text{effective}}$ [GPa]
Non-interaction	16.22
Self-consistent	–
Differential	0.012
Mori-Tanaka	1.78
Levin-Kanaun	–

It is evident that these analytical schemes do not give appropriate results. This can be explained by the fact that basic assumptions following from Eshelby's solution of an ellipsoidal inclusion in an infinite body and required volume fractions are not fulfilled. Still, correct solution has to lie between Voigt and Reuss bounds. Voigt bound [18] describes state when all pores experience same strain when bulk sample is deformed under stress (iso-strain condition) whereas Reuss bound [19] is another extreme assuming that pores experience identical stress when forces are applied to the sample (iso-stress condition). As can be seen in Tab. 2 both bounds are in this case significantly distant from each other:

In the Tab. 1 it can be seen that the non-interaction scheme does not even fulfil the Voigt bound. As self-consistent and Levin-Kanaun schemes lead to zero elastic moduli for porosities lower than porosity of Alporas due to large volume

TABLE 2. Values of Voigt and Reuss bounds

Bound	Young's modulus [GPa]
Voigt	6.02
Reuss	0.0011

fractions of pores (filled with air exhibiting zero mechanical properties), their values in the Table 1 are omitted for convenience. Although differential scheme fulfils the Reuss bound, it leads to substantial underestimation of the actual Young's modulus. Only the Mori-Tanaka scheme ends up close to the nominal elastic modulus $E = 1.4\,\mathrm{GPa}$. Still Mori-Tanaka scheme yields results with notable error. This is caused by the fact that basis of this homogenization scheme is still Eschelby's solution of spherical inclusion in infinite body which is not fulfilled for material with polyhedral pore shapes studied in this paper. The reference value of elastic modulus was obtained using uni-axial compression tests in custom-designed screw-driven loading device by employing digital image correlation method for tracking deformations in the sample [20] in order to eliminate influence of boundary conditions during the measurement.

6. Conclusion

It has been shown that considered analytical homogenization schemes are not suitable for determination of elastic properties of porous materials with this type of microstructure. Only the Mori-Tanaka scheme gives reasonable results but still notably different from reference values. This is in contrast to analytical models derived from percolation theory, where several power- and exponential-law equations yield reasonable and accurate predictions. Instead of analytical schemes presented in this paper, more appropriate numerical homogenization methods employing finite element equivalence of porous microgeometries should be used.

Acknowledgments

The research has been supported by Grant Agency of the Czech Technical University in Prague (grant No. SGS12/205/OHK2/3T/16), research plan of the Ministry of Education, Youth and Sports MSM6840770043, Czech Science Foundation (grant No. P105/12/0824) and by RVO: 68378297.

REFERENCES

[1] *P. Koudelka, O. Jiroušek, J. Valach*, Determination of Mechanical Properties of Metal Foams using Microstructural Models, 10th Youth Symposium on Experimental Solid Mechanics, Chemnitz University of Technology, 2011, 64–65.

[2] *O. Jiroušek, T. Doktor, D. Kytýř, T. Fíla, P. Koudelka, I. Jandejsek, D. Vavřík*, X-ray and finite element analysis of deformation response of closed-cell metal foam subjected to compressive loading, J. Instrum, 2013, in press.

[3] *V. Králík, J. Němeček*, Two-scale model for prediction of macroscopic elastic properties of aluminium foam, Chemické Listy, **106**(2011), 458–461.

[4] *P. Koudelka, O. Jiroušek, T. Doktor, P. Zlámal, T. Fíla*, Comparative study on numerical and analytical assessment of elastic properties of metal foams, Proceedings of Engineering Mechanics 2012, Svratka, 2012, 170–171.

[5] *T. Miyoshi, M. Itoh, S. Akiyama, and A. Kitahara*, Aluminium foam, "ALPORAS": The Production Process, Properties and Applications, Mater. Res. Soc. Symp. P., **521**(1998).

[6] *K. Bobzin, E. Lugscheider, R. Nickel, T. Kashko*, Advanced homogenization strategies in material modeling of thermally sprayed TBCs, Adv. Eng. Mater., **8**(2006), No. 7, 663-669.

[7] *G. Laschet et al.*, Microstructure based model for permeability predictions of open-cell metallic foams via homogenization, Mat. Sci. Eng. A-Struct., **472**(2008), 214-226.

[8] *V. J. Laraja, I. L. Rus, A. H. Heuer*, Microstructural Shape Factors: Relation of Random Planar Sections to Three-Dimensional Microstructures, J. Am. Ceram. Soc., **78**(1995), 1532–1536.

[9] *O. Eroshkin, I. Tsukrov*, On micromechanical modeling of particulate composites with inclusions of various shapes, Int. J. Solids Struct., **42**(2005), 409–427.

[10] *I. Sevostianov, M. J. Kachanov*, Explicit cross-property correlations for anisotropic two-phase composite materials, Mech. Phys. Solids, **50**(2002), 253–282.

[11] *I. A. Kunin*, Elastic Media with Microstructure, Springer Verlag, Berlin, 1983.

[12] *I. Sevostianov, J. Kováčik, F. Simančík*, Elastic and electric properties of closed-cell aluminum foams: Cross property connection, Mat. Sci. Eng. A-Struct., **420**(2006), 87-99.

[13] *A. Zaoui*, Continuum Micromechanics: Survey, J. Eng. Mech. **128**(2002), No. 8, 808–816.

[14] *K. Z. Markov*, in: K. Z. Markov, L. Preziozi (Eds.), Heterogeneous Media: Micromechanics Modeling Methods and Simulations, Birkhauser, Boston, 2000.

[15] *R. W. Zimmerman*, Elastic moduli of a solid containing spherical inclusions, Mech. Mater., **12**(1991), 17–24.

[16] *Y. Benveniste*, On the Mori-Tanaka's method in cracked bodies, Mech. Res. Commun., **13**(1986), 193–201.

[17] *V. M. Levin*, On the determination of the effective elastic moduli of composite materials, Dokl. Akad. Nauk SSSR, **220**(1975), 1042-1045.

[18] *W. Voigt*: Lehrbuch der Kristallphysik, Teubner, Berlin, 1928.

[19] *A. Reuss*: Berechnung der fliegrenze von mischkristallen auf grund den konstanten des einkristalls, Z. Angew. Math. Mech., **9**(1929), 49.

[20] *I. Jandejsek, D. Vavřík*: Experimental measurement of the J-Integral using digital image correlation method, 18th European Conference on Fracture: Fracture of Materials and Structures from Micro to Macro Scale, 2010, 184–189.